International Journal of Engineering Inventions
e-ISSN: 2278-7461, p-ISSN: 2319-6491
Volume 13, Issue 4 [April. 2024] PP: 81-90

Research on finite element simulation and parameter optimization of milling stainless steel with micro-textured ball end milling cutter

Baizhong Wang- Kai Xiao- Hu Shi
School of Mechanical and Vehicle Engineering, Changchun University, Changchun 130022, China

***Abstract**: In order to improve the cutting performance of cutting tools in metal cutting, a micro-texture tool is proposed in this paper, and micro-texture diameter, width, spacing and edge distance are set as four parameters. The three-dimensional model of micro-texture tool is established and the cutting process is simulated by finite element simulation. The influence of cutting force and cutting temperature on the performance of the tool is studied. Orthogonal test is carried out to analyze the milling force and milling temperature and study the influence of different micro-texture parameters on the milling performance of the tool and obtain the parameters that have the greatest influence on the milling performance of the tool. The results show that the micro-texture tool can effectively improve the cutting performance of the tool. When the micro-texture diameter is 69.8873μm, the micro-texture width is 40.0001μm, the micro-texture spacing is 100.0000μm, and the edge distance is 117.7327μm, the milling performance of the tool is the best.*

Keywords: combined micro-texture, milling performance of the tool, milling force, milling temperature, Parameter optimization

---

Date of Submission: 02-04-2024 Date of acceptance: 12-04-2024

I. INTRODUCTION

304 stainless steel is widely used in various fields, but its own mixed with a variety of elements will also affect its processing performance. In the process of cutting, the main performance is large cutting force, and high cutting temperature [1,2]. Domestic and foreign scholars have found through a large number of studies that the cutting performance of new tools with micro-texture is better than that of ordinary tools [3]. Chen, P et al studied the effect of cutting speed on the surface quality of hardened bearing steel GCr15 in dry turning with micro-texture PCBN tool. The research results show that the effect of cutting speed on surface roughness varies with different micro-texture types. [4]. Zhang Qing ge took machining cutting force as the main optimization index and optimized the cutting consumption of 304 stainless steel by orthogonal experiment and finite element simulation [5]. Fang Rui et al. studied the evolution law of cutting force with machining parameters by single factor experiment. Research shows that the cutting force decreases first and then increases with the increase of spindle speed, and increases with the increase of feed rate and cutting depth [6]. Xu et al. obtained the relationship model and correlation between process parameters and cutting force through comparative experiments of turning. The results show that the cutting depth has a great influence on the cutting force [7]. Sahu,A.K., et al studied the hybrid fabrication of AISI316L. The research results show that different structural characteristics lead to differences in the machinability of materials [8]. Kishawy HossamA verified the model through the orthogonal cutting test of AISI1045 steel pipe. The results showed that the optimal micro-texture design eliminated the derivative cutting. [9]. Patel Kaushalandra takes carbide cutting tools as the research object to explore the influence of micro-texture geometric parameters on cutting performance, and the research shows that the cutting performance of the texture tool is related to the change of its parameters [10].

Therefore, in order to improve the cutting performance of the tool, this paper uses finite element simulation to simulate the cutting process, studies the influence of micro-texture on the cutting performance of the tool through the changes of force and temperature, and finally establishes a mathematical model, optimizes the parameter size and obtains the optimal parameter combination according to the genetic algorithm.

1 FINITE ELEMENT MODEL ESTABLISHMENT

1.1 Design of micro-texture model

At present, the research of many scholars at home and abroad shows that pitting micro-texture and grooving micro-texture can better improve the cutting performance of the tool and extend the service life of the tool compared with most micro-texture types in the field of tool cutting.

Therefore, considering the good effect of pit micro-texture and groove micro-texture in improving the cutting performance of the tool, this paper designed two shapes of pits and grooves, and two combined shapes of pits and grooves as the micro-texture of the ball end milling cutter blade surface. Four micro-texture models are designed, as shown in Figure 1.

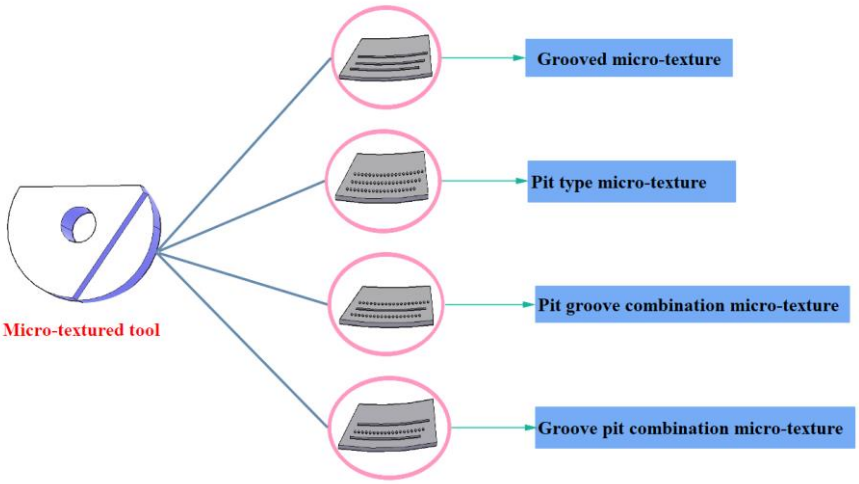

Fig.1. *Distribution of micro-texture types*

1.2 3D model establishment

Before the finite element simulation of the cutting process of the tool, the 3D models of the tool and the workpiece are first established. In order to explore the performance differences of the combined micro-texture, the single micro-texture tool and the non-texture tool, four different 3D models of the tool are established based on the concave texture and the groove texture, in order to reduce the calculation amount of the finite element simulation and ensure the calculation accuracy. The tool model is simplified reasonably. During the establishment of the finite element simulation tool model, different types of micro-textures were placed on the front and back surfaces of the milling cutter blades, and the ball-end milling cutter model was established, as shown in Figure 2:

Fig.2. *3D model of ball end milling cutter*

1.3 Constitutive model established

In cutting simulation, Johnson-Cook constitutive model fully considers the relationship between flow stress and strain, strain rate and temperature, and can be used to simulate deformation under dynamic loads, such as impact loads, to meet the requirements of simulation materials under various conditions. Therefore, the material constitutive model in this finite element simulation is selected as Johnson-Cook constitutive model, and its empirical formula is:

$$\sigma = \left[A + B(\varepsilon)^n \right] \bullet \left[1 + C\ln\left(\frac{\dot{\varepsilon}_p}{\dot{\varepsilon}_0} \right) \right] \left\{ 1 - \left(\frac{t - t_0}{t_m - t_0} \right)^m \right\} \quad \textbf{(1)}$$

Among them; σ —material flow stress, A —material yield limit, B—strain change coefficient, c m n—material characteristic coefficient, ε—Equivalent plastic strain, p—equivalent plastic strain rate, 0—reference value of strain rate, t —deformation temperature, t_0 —room temperature, t_m —material melting point temperature.

The workpiece material of this finite element simulation is 304 stainless steel, and the parameters of its constitutive model are set as shown in Table 1:

Table 1. Johnson-Cook constitutive model parameters of 304 stainless steel

A(MPa)	B(MPa)	C	m	n	T_0
240	695	0.0141	0.945	0.795	25

II. THE FIRST STAGE OF FINITE ELEMENT SIMULATION TEST

2.1 The first stage of finite element simulation test design

In the first stage of the finite element simulation test, the milling test without texture tool was taken as the control, the processing conditions remained unchanged, and the finite element simulation plan was set as shown in Table 2.

Table 2. First stage finite element simulation schedule

Test No.	micro-texture type	position
1	no texture	no
2	pit	rake face
3	pit	flank face
4	groove	rake face
5	groove	flank face
6	pit-groove-pit	rake face
7	pit-groovet-pit	flank face
8	groove - pit - groove	rake face
9	groove - pit - groove	flank face

The influence of micro-texture on milling force and milling temperature was investigated by finite element simulation experiments in this stage. The influence of micro-texture on milling force of different surfaces and the influence of combined texture compared with a single type of texture on cutter milling force were explored. At the same time, the micro-texture type with the best milling effect was selected according to the average milling force and milling temperature of the tool for subsequent research.

2.2 The first stage of finite element simulation milling force analysis

According to the calculation results of the finite element simulation, the variation diagram of the milling force in three directions is drawn by the drawing tool, as shown in Figure 3

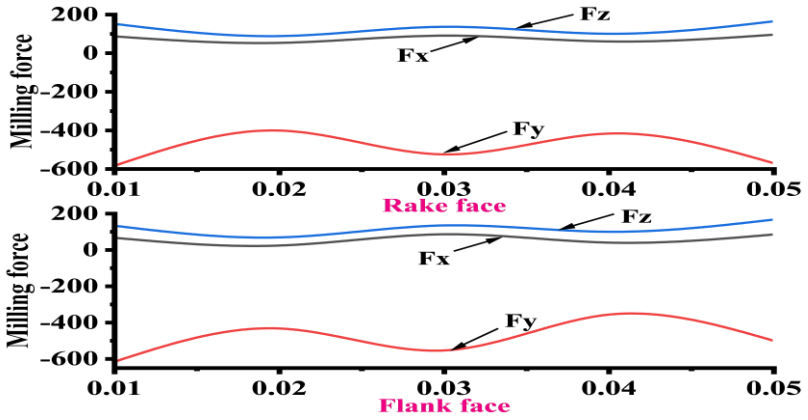

Fig.3. *Milling force variation diagram*

Through the data graphs of each group of simulation milling force tests, it can be clearly seen that in the milling force of ball end milling cutter in three directions during milling process, the milling component force along the feed direction of the tool and the milling component force perpendicular to the feed direction change gently, and the milling force value is small. The milling component force of the milling cutter along the axial direction of the milling cutter fluctuates greatly, and the value of the force is much greater than that of the milling component in the other two directions. Analyzing the reasons, the cutting area of the cutter will increase with the increase of cutting depth and width, which leads to the need for greater tangential force and radial force to overcome the cutting strength of the material. Therefore, the tangential and radial forces of the tool will increase with the increase of the depth and width of the milling. The milling depth adopted in this test is small,

so the tangential and radial forces of the milling cutter are small.

The simulation milling force data is processed and the milling force resultant is calculated for reference. The change of milling force when drawing different types of micro-texture distributed on different surfaces of the tool is shown in Figure 4, It can be intuitively seen from the figure that due to the existence of micro-texture on the tool surface, the milling force generated by the ball end milling cutter is significantly reduced, and when the same type of micro-texture is on different surfaces of the tool, the effect of reducing the milling force is small, and the milling force of the tool with micro-texture placed in the back tool surface is slightly higher than that of the micro-texture in the front tool surface, compared with a single type of micro-texture. The milling force generated by the grooved, recessed and recessed micro-textured tools placed on the front tool surface is the least, while the milling force generated by the grooved and recessed micro-textured tools placed on any surface of the tool is much greater than that generated by other types of micro-textured tools.

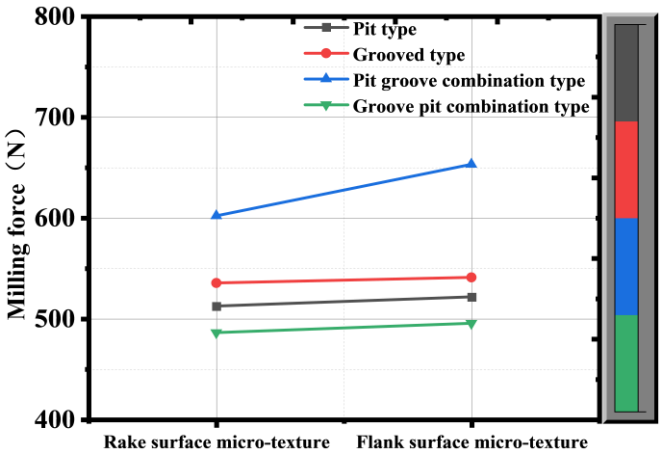

Fig.4. *Variation of milling force for different types of micro-textures on different surfaces of the tool*

2.3 The first stage of finite element simulation milling temperature analysis

In order to conduct a macroscopic analysis of the surface temperature of different types of micro-texture tools in different placement positions during milling, this section extracts the surface temperature of the tools in the entire milling process from the time when the ball end milling cutter cuts into the workpiece to the workpiece cutting, and analyzes the temperature curve changes of milling 304 stainless steel with different types of micro-texture ball end milling cutters placed on different tool surfaces. At the same time, comparing with the non-woven ball end milling cutter, observing the temperature cloud diagram of the tool in the milling process as shown in Figure 5, it can be clearly observed that the temperature distribution state of the surface of each tool has a certain regularity, that is, the highest temperature area of the tool is concentrated in the vicinity of the cutting edge of the ball end milling cutter. Therefore, the analysis of the tool surface temperature in the finite element simulation process adopts node temperature analysis. Five NT nodes were selected at the cutting edge parts of nine groups of tools to replace the overall temperature of the tool, and the final average milling temperature was calculated for subsequent reference. The milling temperature generated by different tools in the milling process was drawn into a point plot, as shown in Figure 6.

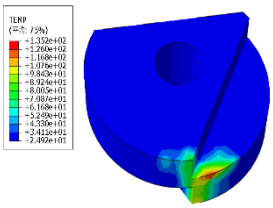

Fig. 5. *Temperature field simulation cloud image*

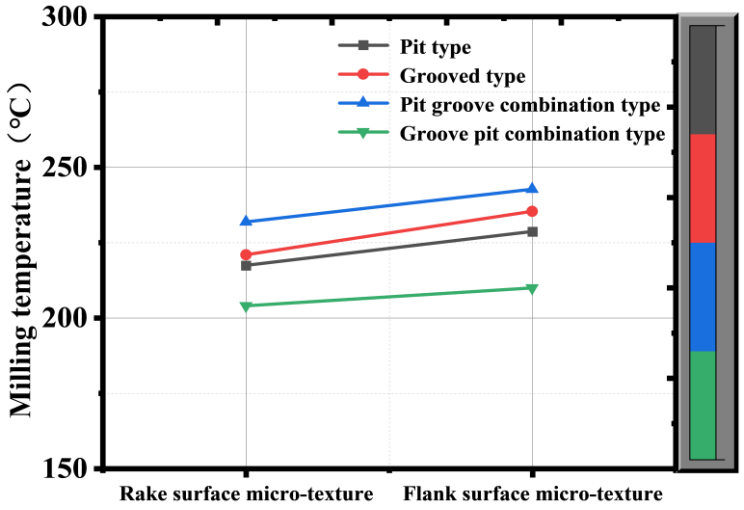

Fig. 6. *Variation of milling temperature for different types of micro-textures on different surfaces of the tool*

According to the calculation results, the change of milling temperature when different types of micro-textures are distributed on different surfaces of the tool is shown in the figure. It can be intuitively seen from the figure that the milling temperature generated by the ball end milling cutter is significantly reduced due to the existence of micro-textures on the surface of the tool, and when the same type of micro-textures are on different surfaces of the tool, their ability to reduce milling temperature is small. In addition, the milling temperature of the tool with micro-texture embedded in the back tool surface is slightly higher than that of the tool with micro-texture in the front tool surface. Compared with the single type of micro-texture, the milling temperature of the tool with groove-pit-groove combination micro-texture embedded in the front tool surface is the smallest. However, the milling temperature of the pit-groove-pitted micro-texture structure placed on any surface of the tool is much higher than that of other types of micro-texture tools. By observing the temperature field of the tool surface, with the increase of the distance between the position of the tool surface and the cutting edge, the surface temperature has a significant phenomenon of gradual decrease. Moreover, compared with the area where the tool and the workpiece friction each other, the temperature field in the area where the tool and the chip contact each other changes more violently. By analyzing the temperature comparison diagram of the tool surface, the tool surface temperature of the same type of micro-texture ball end milling cutter with micro-texture placed in the back tool surface is about 15°C higher than that of the tool with micro-texture placed in the front tool surface. The reason is that embedding micro-texture in the front tool surface can not only effectively reduce the friction between the tool and the chip, but also, Due to the existence of micro-texture, the area of heat conduction is increased and the friction heat generation of the tool is reduced. In the first stage of the finite element simulation, the simulation milling force and milling temperature of the front micro-texture tool, the back micro-texture tool and the non-texture tool are compared, and it is found that the cutting performance and cooling effect of the micro-texture tool are obviously better than that of the non-texture tool. At the same time, when the groove-pit groove-type micro-texture is placed on the front tool surface, the milling force on the tool is the smallest and the milling temperature is the lowest. Therefore, the groove-pit groove-type micro-texture is taken as the main research object of the follow-up test, and different micro-texture parameters are designed for follow-up research.

III. THE SECOND STAGE OF FINITE ELEMENT SIMULATION TEST

3.1 The second stage of finite element simulation test design

In the second stage of finite element simulation test, micro-texture parameters were designed according to the micro-texture types selected in the first stage, and the changes of cutter milling force and milling temperature with the change of the size of the same micro-texture parameters were explored, as well as the degree of influence of different micro-texture parameters on the milling force of the tool was explored, and the basis was laid for the final selection of the optimal combination of micro-texture parameters. According to the designed micro-texture structure, micro-texture diameter, micro-texture width, micro-texture spacing and edge distance are selected as the four parameters of micro-texture, and nine three-dimensional models of ball-end milling cutter are established. Meanwhile, four-factor and three-level orthogonal tests are designed. The factors and levels table are shown in Table 3.

Table 3 . Factors and levels

	Diameter (μm)	Width (μm)	Spacing (μm)	Edge distance (μm)
Level 1	50	40	80	100
Level 2	60	50	90	110
Level 3	70	60	100	120

3.2 The second stage of finite element simulation milling force analysis

The resultant force of milling forces in three directions was calculated, and the average milling force in the overall milling process was calculated as a reference. The range difference of each parameter was calculated through the software and compared, as shown in Table 4. Using the data after range analysis, the point plot of the changing trend of milling force with different micro-texture parameters at different levels is drawn, as shown in Figure7.

Table 4. Milling force analysis data

	Diameter (μm)	Width (μm)	Spacing (μm)	Edge distance (μm)
Level 1	522.233	500.233	534.367	582.867
Level 2	446.933	429.800	507.633	438.333
Level 3	526.733	565.867	453.900	474.700
R	79.800	136.067	80.467	144.534
Rank	4	2	3	1

Through the range analysis of milling force, it can be found that the order of influence of several experimental parameters on milling force is as follows: edge distance > micro-texture width > micro-texture spacing > micro-texture diameter. The data after range analysis is drawn into a point plot.

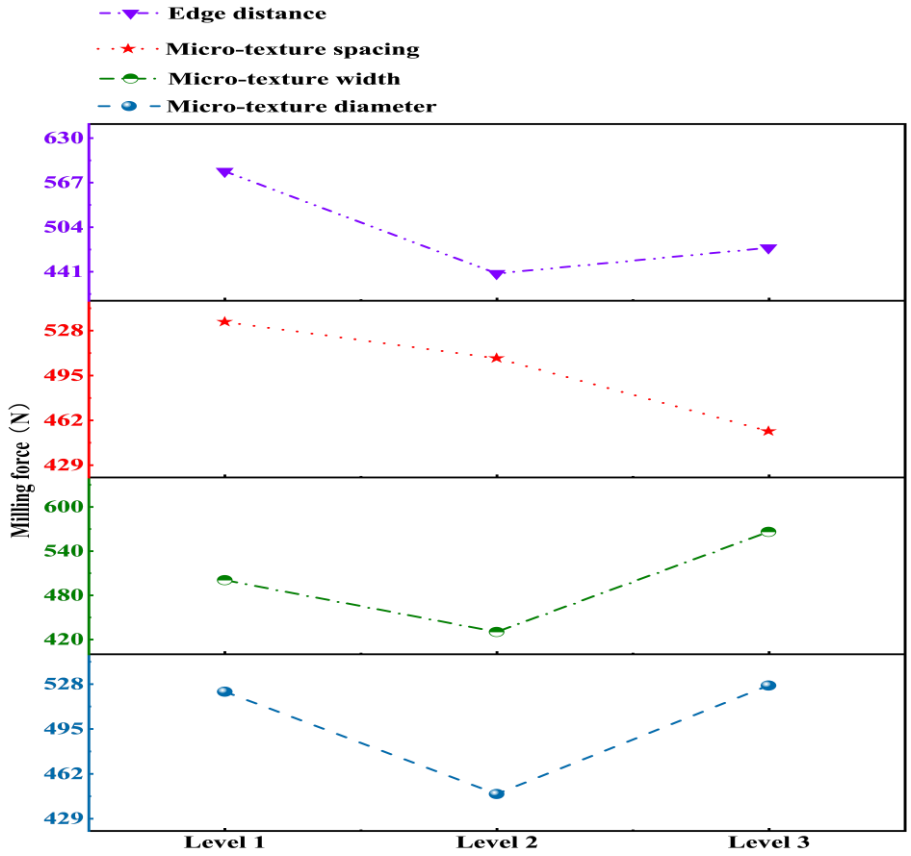

Fig. 7. *Relation between micro-texture characteristic parameters and milling force*

As shown in the figure, the four parameters of the micro-texture were analyzed separately. As the diameter and width of the micro-texture increased, the milling force decreased first and then increased. When the micro-texture diameter was 60μm, the milling force was the smallest and the effect of the micro-texture was the best; when the micro-texture diameter increased to 70 μm, the milling force reached the maximum. When the micro-texture width is 50 μm, the milling force reaches the minimum value, and when the width increases to 60μm, the milling force reaches the maximum. The changing trend of milling force along with the diameter and width of the micro-texture shows that the friction contact area between the tool and the chips can be reduced by placing pits and grooves of appropriate size, which can further control the size of the friction force. It also shows that whether the size of the micro-texture is reasonable directly affects the ability of the micro-texture to hold chips. The milling force decreases first and then increases with the distance between the micro texture and the edge. According to the change trend of the distance between the micro texture and the edge on the milling force, when the milling force reaches the relative minimum value, the distance between the micro texture and the edge is 110 μm, and when the edge distance is 100 μm, the milling force reaches the maximum. With the increase of the distance from the edge, the micro-texture can reduce the milling force, but with the gradual increase of the distance from the edge, the number of micro-textures that can continue to play a role becomes less and less, and thus the milling force increases. With the increasing of micro-texture spacing, the stress concentration on the surface of the tool is alleviated, and the effect of micro-texture on reducing milling force and improving milling performance is shown, so that the milling force shows a trend of decreasing gradually. And when the micro-texture spacing increases to 100 μm, the milling force on the tool is the least.

3.3 The second stage of finite element simulation milling temperature analysis

Through observation and analysis of the cloud map of temperature field changes in the simulation results of each group of orthogonal simulation tests, the node temperature when the tool enters the stable milling state is extracted, and the data is sorted and calculated to obtain the average milling temperature during the milling process. At the same time, orthogonal design software was used to carry out range analysis on the simulation results of milling temperature, and the analysis results were shown in Table 5. The level data of each factor in the milling temperature range analysis table were divided into point plots, as shown in Figure 8, and then the influence of micro-texture parameters on milling temperature at different levels and the influence degree of different micro-texture parameters on cutter milling temperature were analyzed.

Table 5. Milling temperature analysis data

	Diameter (μm)	Width (μm)	Spacing (μm)	Edge distance (μm)
Level 1	261.88	241.27	267.81	266.69
Level 2	226.04	214.51	239.68	218.61
Level 3	251.29	283.43	231.72	253.90
R	35.84	68.92	36.09	48.09
Rank	3	1	4	2

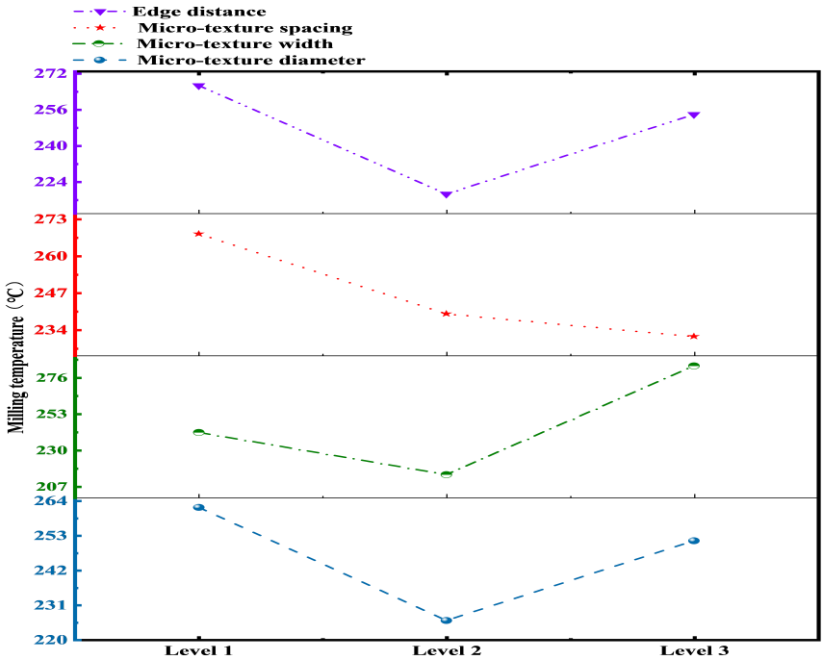

Fig. 8. *Relation between micro-texture characteristic parameters and milling temperature*

According to the range table, among the four parameters of micro-texture set, the influence of micro-texture width on milling temperature occupies a major position, and the distance between micro-texture and cutting edge also has a great influence on milling force. The order in which the micro-texture parameters affect the milling temperature is as follows: micro-texture width > edge distance > micro-texture diameter > micro-texture spacing. It can be seen from the point plot that with the increase of the micro-texture width, the milling temperature presents a trend of decreasing first and then increasing. When the micro-texture width increases to 50μm, the micro-texture has the best effect on reducing the milling temperature. This is because under the same heat transfer condition, when the micro-texture width changes, the hollow structure will have certain changes. The diffusion of heat generated in the milling process will have a certain delay, the heat dissipation efficiency of the cutter body is low, and when the width is too large, the ability to accommodate chips in the space is strong, and at the same time, the heat can not be effectively dissipated, and the milling temperature rises more vigorously. The milling temperature decreases first and then increases with the distance between the micro-texture and the edge. According to the change trend of the distance between the micro-texture and the edge on the milling force, when the milling temperature reaches the relative minimum value, the distance between the micro-texture and the edge is 110μm, and when the edge distance is 100μm, the milling temperature reaches the maximum. With the increase of the distance from the edge, the existence of micro-texture can play a role in reducing the milling temperature, but with the gradual increase of the distance from the edge, the contact area between the micro-texture area on the tool surface and the workpiece gradually decreases, so that the micro-texture can not play its role. With the increasing of micro-texture spacing, the milling temperature showed a decreasing trend. When the micro-texture spacing was 100μm, the milling temperature of the tool reached the highest level.

IV. PARAMETER OPTIMIZATION

4.1 Mathematical model establishment

According to the four micro-texture parameters set, the micro-texture diameter, micro-texture width, micro-texture spacing and edge distance are taken as independent variables in the mathematical model, and the milling force and milling temperature are taken as optimization objectives. Due to the complexity of the process of solving the computational nonlinear equation, the nonlinear equation must first be transformed into a linear equation, and the model structure is shown as follows

$$S = KA^{a_1}B^{a_2}C^{a_3}D^{a_4} \tag{2}$$

In the formula, S represents the optimization objective, K represents the correlation coefficient with material properties, and A, B, C, and D represent micro-texture diameter, micro-texture width, micro-texture spacing and edge distance respectively. a_1, a_2, a_3, a_4 are correction factors.

Take logarithms of both sides of the above equation at the same time to get the formula as shown in the equation.

$$\ln S = \ln K + a_1 \ln A + a_2 \ln B + a_3 \ln C + a_4 \ln D \tag{3}$$

Set lnS=y, lnK=a_0, lnA=x1, lnB=x_2, lnC=x_3, lnD=x_4, and the corresponding linear regression equation is shown as follows:

$$y = a_0 + a_1x_1 + a_2x_2 + a_3x_3 + a_4x_4 + \varepsilon \tag{4}$$

In the formula, y represents the evaluation index of the test, x_1, x_2, x_3, x_4 represents the four variables of the test, and ε is the test error. The linear equations are established according to the milling force and milling temperature data obtained by nine sets of simulated orthogonal tests.

$$\begin{aligned} y_1 &= a_0 + a_1x_{11} + a_2x_{12} + a_3x_{13} + a_4x_{14} + \varepsilon_1 \\ y_2 &= a_0 + a_1x_{21} + a_2x_{22} + a_3x_{23} + a_4x_{24} + \varepsilon_2 \\ &\cdots\cdots \\ y_9 &= a_0 + a_1x_{91} + a_2x_{92} + a_3x_{93} + a_4x_{94} + \varepsilon_9 \end{aligned} \tag{5}$$

The linear equations are expressed in matrix form as follows:

$$Y = Xa + \varepsilon \tag{6}$$

The multivariate linear equations are expressed in matrix form as:

$$a = (X^TX)^{-1}X^TY \tag{7}$$

Where X^T is the transpose of X and the inverse of $(X^TX)^{-1}$.

The milling force, milling temperature results of the finite element simulation and micro-texture parameters of each group of tests were respectively brought into the above formula, and calculated by MATLAB software. Finally, the regression model of milling force was obtained:

$$F = e^{7.5111} A^{-0.0052} B^{0.0008} C^{-0.0078} D^{-0.0035} \quad (8)$$

The milling temperature regression model is obtained as follows:

$$T = e^{6.0639} A^{-0.0017} B^{0.0087} C^{-0.0078} D^{-0.0018} \quad (9)$$

4.2 Optimization results of micro-texture parameters

In this paper, genetic algorithm is used to optimize micro-texture parameters. Genetic algorithm is an iterative optimization algorithm based on the principle of natural selection, and its algorithm flow is shown in Figure 9.

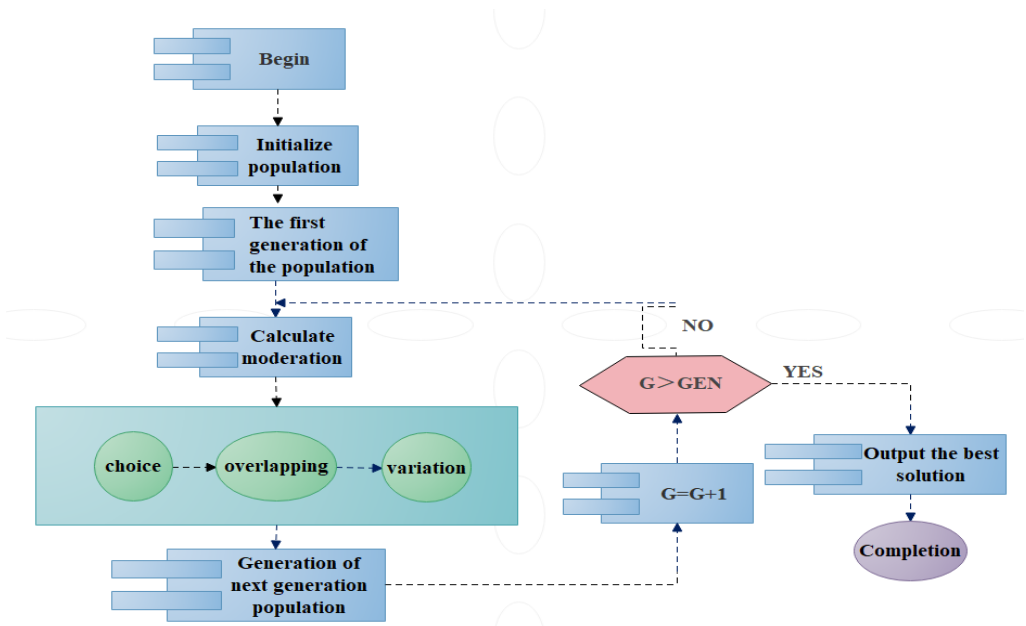

Fig. 9. *Genetic algorithm flow*

the optimal solution is: The micro-texture diameter is 69.8873 μm, the micro-texture width is 40.0001 μm, the micro-texture spacing is 100.0000 μm, and the edge distance is 117.7327 μm.

V. Conclusions

The conclusions were as follows:

1) In the milling process, compared with non-texture tools, micro-texture tools can effectively improve the cutting performance of the tool.

2) Under the same cutting conditions, comparing the four parameters of micro-texture, it is found that the order of influence on milling force is: edge distance > micro-texture width > micro-texture spacing > micro-texture diameter. the order of influence on milling temperature is: micro-texture width > edge distance > micro-texture diameter > micro-texture spacing.

4) Genetic algorithm was used to optimize the parameters through the control experiment: when the micro-texture diameter is 69.8873 μm, micro-texture width is 40.0001 μm, micro-texture spacing is 100.0000 μm, edge distance is 117.7327 μm, the milling performance of the tool is the best.

REFERENCES

[1]. Ezugwu EO. (2005) Key improvements in the machining of difficult-to-cut aerospace superalloys. International Journal of Machine Tools and Manufacture;45:1353-1367.

[2]. Ding H, Shen N, Shin YC. (2011) Thermal and mechanical modeling analysis of laser-assisted micro-milling of difficult-to-machine alloys. Journal of Materials Processing Tech.;212:601-613.

[3]. A. SS, Amlan K, Kishore MK, Adepu K. (2023) Enhancement of microstructure, micro-texture, and mechanical properties of Al6061 friction stir welds using the developed static shoulder welding tool. Materials Characterization;203.

[4]. Pan C, Li Q, Hu K, Jiao Y, Song Y. (2018) Study on Surface Roughness of Gcr15 Machined by Micro-Texture PCBN Tools. Machines;6:42-42.

[5]. Zhang Qingge. Optimization of cutting parameters and finite element simulation for surface milling austenitic stainless steel [master]; 2013.

[6]. Fang Rui, Zou Ping, DUAN Jingwei, WEI Shiyu. (2023) Experimental study on anti-friction characteristics and surface quality of three-dimensional ultrasonic vibration assisted turning. Journal of Northeastern University (Natural Science Edition);44:233-241.

[7]. Yingshuai X, Zhihui W, Ping Z, Weili H, Guoqing Z. (2021) Experimental study on cutting force in ultrasonic vibration-assisted turning of 304 austenitic stainless steel. Proceedings of the Institution of Mechanical Engineers;235:494-513.

[8]. Kumar SA, Sunil J. (2022) Hybrid laser and micro milling methods for higher depth microchannel fabrication. Journal of Manufacturing Processes;81:672-679.
[9]. A. KH, Amr S, Hussien H, Ali H, Mohamed E. (2022) An analytical model for the optimized design of micro-textured cutting tools. CIRP Annals - Manufacturing Technology;71:49-52.
[10]. Kaushalandra P, Guoliang L, R. SS, Tuğrul Ö. (2020) Effect of Micro-Textured Tool Parameters on Forces, Stresses, Wear Rate, and Variable Friction in Titanium Alloy Machining. Journal of Manufacturing Science and Engineering;142.